SAND2020-10893C

# 2D microstructure reconstruction for SEM via non-local patch-based image inpainting

Anh Tran * and Hoang Tran

**Abstract** Microstructure reconstruction is a long-standing problem in experimental and computational materials science, for which numerous attempts have been made to solve. However, the majority of approaches often treats microstructure as discrete phases, which in turn, reduces the quality of the resulting microstructures and limits its usage to the computational level of fidelity, but not the experimental level of fidelity. In this work, we applied our previously proposed approach [43] to generate synthetic microstructure images at the experimental level of fidelity for the UltraHigh Carbon Steel DataBase (UHCSDB) [13].

## 1 Introduction

Microstructures are a crucial link between process and property, encoding nearly all information related to the processes used to manufacture the specimen. However, microstructures are naturally complicated to study due to its spatial stochasticity, which varies from one location to another, within certain bounds, usually referred to as aleatory uncertainty. This, in turn, leads to the concept of statistically equivalent microstructure, where the microstructure features are either deterministically or statistically measurable by microstructure descriptors, which are the key enablers for microstructure reconstruction and generation problems. While most of microstructure reconstruction and microstructure generation problems are already very well solved in the context of computational materials science, only a few attempts to generate and reconstruct microstructures that are equivalent to experimental level, such as images obtained from using scanning electron microscope, have been made.

Microstructure reconstruction and generation at the experimental level are high-fidelity, because images are represented in either RGB or grayscale. It is fairly straightforward to threshold a RGB or grayscale image to produce a computational microstructure, which is a usual representation of phase-based microstructures for integrated computational materials engineering (ICME) workflow. However, it is nearly impossible to perform an inverse threshold to convert a binary or any phase-based microstructure back to a RGB or grayscale image, which is often a product of scanning electron microscope (SEM) or transmission electron microscope (TEM). The problem of microstructure reconstruction and microstructure generation at the level of experiment is mainly unsolved. However, its importance is found due to the scarcity of experimental materials data, which is well-known to be resource-intensive, i.e. human labor, time, and money [2].

There are mainly two approaches for this problem: the first one is based on machine learning (ML) / deep learning (DL) techniques, whereas the second one is based on conventional image processing techniques, which does not employ DL. While DL has been touted as a revolutionary technique to solve many problems, the lack of data repositories for experimental microstructures poses a significant challenge towards the adoption and application of DL in materials science in general. Notably, convolutional neural networks (CNN), including generative adversarial network (GAN) [20], are among popular choices for DL.

For example, Bostanabad [5] adopted VGG19 [36] to reconstruct 3D microstructure from 2D images using transfer learning. Iyer et at. [24] employed an auxiliary classifier Wasserstein GAN with gradient penalty to generate microstructure from UHCSDB, which is the same dataset considered in this work. Singh et al. [37] used Wasserstein GAN to generate and reconstruct microstructure with

Anh Tran
Center of Computing Research, Sandia National Laboratories, Albuquerque, NM. e-mail: anhtran@sandia.gov

Hoang Tran
Computer Science and Mathematics Division, Oak Ridge National Laboratory, Oak Ridge, TN. e-mail: tranha@ornl.gov

* Corresponding author: e-mail: anhtran@sandia.gov

binary phases. DeCost et al. [12] applied VGG16 and t-SNE [31, 15] to visualize microstructure on their latent manifold space. DeCost et al. [14] applied a pre-trained VGG16 [36] for deep semantic segmentation in the same UHCSDB dataset. Ling et al. [29] also used VGG16 to extract features for SEM images between different datasets in the hope of generalization and interpretation. Li et al. [28] employed an auto-encoder (AE) approach to generate microstructures. Chun et al. [11] employed GAN to generate microstructures and showed that GAN is able to generate better quality images compared to AE, which is a well-known problem in computer vision. Mosser et al. [32] proposed a GAN to generate microstructure. Cang et al. [7, 8] employed deep belief network in reconstructing binary microstructure. Bostanabad et al. [6] proposed a tree-based ML technique for 2D stochastic microstructure reconstruction based on classification trees.

Zichenko [54] proposed an isotropic algorithm for random close packing of equisized spheres with periodic boundary conditions. Groeber et al. [23, 21, 22] proposed an automatic statistical framework to characterize [21] and to create statistically equivalent synthetic microstructures [22]. Fullwood et al. [19, 18] proposed a phase-recovery algorithm based on two-point correlation statistics to reconstruct the microstructure. Latief et al. [25] suggested a stochastic geometrical modeling approach to generate a $\mu$-CT images of Fontainebleau sandstone. Staraselski et al. [38] demonstrated the application of two-point correlation function in constructing 3D representative volume element. Feng et al. [17] proposed a stochastic microstructure reconstruction for two-phase composite materials based on nonlinear transformation of Gaussian random fields that matches the marginal probability distribution function and the two-point correlation function. Chen et al. [9] employed simulated annealing method to reconstruct 3D multiphase microstructure and demonstrated with 2D and 3D reconstruction with three-phase sandstone. Xu et al. [52, 53] proposed a descriptor-based methodology using multiple microstructure descriptors as evaluation criteria to reconstruct 3D microstructure. Chen et al. [10] proposed a multiscale computational scheme to stochastically reconstruct the 3D heterogeneous polycrystalline microstructure from a single 2D electron back-scattered diffraction (EBSD) micrograph. Li et al. [27, 26] conducted a comparison study on the effects of multiple objectives in the microstructure reconstruction problem.

In this paper, we adopt our previous approach [43], which is extended based on Newson et al. [34], using non-local patch-based image inpainting to produce texturally coherent microstructures and demonstrate its usage on UHCSDB [13]. The remaining of the paper is organized as follows. Section 2 presents the image inpainting methodology that is extensively used as a basic tool in this work. Section 3 presents the numerical demonstration on the publicly available UHCSDB dataset [13]. Section 4 discusses and concludes the paper.

## 2 Image inpainting

The algorithm for image inpainting is described in details from our previous work [43], where we augment the algorithm from Newson et al. [34] for solving microstructure inpainting problems. For the sake of completeness, we briefly summarize the algorithm here. This line of research has been gradually developed and improved over years [33, 16, 34], where the PatchMatch algorithm [3] was employed to accelerate the nearest neighbor search. Figure 1 shows a schematic of the image inpainting problem, where image patches are denoted as gray squares, $\mathcal{H}$ is the occluded region to be inpainted, and $\mathcal{D}$ is the unoccluded region.

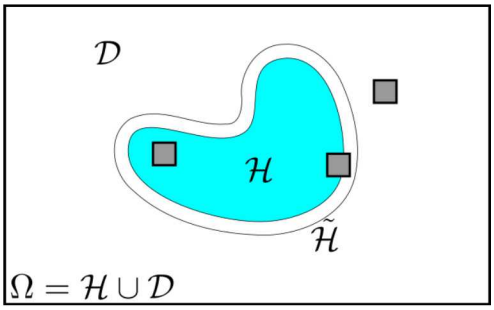


Fig. 1: Schematic of image inpainting problem, where the patches can be unoccluded, partially or completely occluded. Reprinted with permission from [43].

In patch-based inpainting approach, we fill in the missing region patch-by-patch by looking for well-matching replacement patches in the unoccluded part of the image and copying them to corresponding locations. In other words, let $u$ be the image content and $W_p$ be the image patch at position $p$, we find the map $\phi$ that locates its nearest neighbor $W_{p+\phi(p)}$, i.e., image patch in $\mathcal{D}$ that is most similar to $W_p$. We need to do this for every position $p$ in $\mathcal{H}$, therefore, the image reconstruction problem involves minimizing

$$E(u, \phi) = \sum_{p \in \mathcal{H}} d^2(W_p, W_{p+\phi(p)}). \tag{1}$$

Here, $d$ is a distance function formalizing the similarity between patches, [39, 30]. Unfortunately, (1) is an nonconvex, NP-hard optimization problem. To overcome this challenge, we adopt an iterated alternating approach. Specifically, we break the minimization of (1) into two separate minimization problems with respect to the shift map $\phi$ and the image content $u$, which are solved alternatively

in iterations (see Algorithm 1). These two problems correspond to a nearest neighbor search and an image reconstruction process accordingly.

For the **nearest neighbor search**, as in [34], only approximate, instead of exact, nearest neighbors (NN) are computed, due to the demanding cost of the later one. We use PatchMatch algorithm by Barnes et al. [3] for this goal. The process is initialized by randomly assigning each occluded pixel a candidate nearest neighbor in the unoccluded region. Then, for each iteration, each pixel is visited in lexicography order (on even iterations) and in inverse lexicography order (on odd iterations). At each pixel, we perform two operations for improving the shift map $\phi$. First, we check the nearest neighbors of the adjacent pixels for better candidate nearest neighbor of the current pixel; and second, we look for better nearest neighbor at random in an increasingly small window around the current nearest neighbor. For more details, the readers are referred to the seminal work on PatchMatch algorithm [3]. The PatchMatch pseudo-code for minimization with respect to $\phi$ is given in Algorithm 2 and can also be found in [3, 16, 43].

**Algorithm 1** Minimization of $E(u, \phi)$ via iterated alternating approach. Reprinted with permission from [43].

**Input:** Initial guess $u_0$ and tolerance $\tau > 0$
**Output:** Inpainted image $u_{k+1}$

1: **repeat**
2: $\phi_k \leftarrow \arg\min_{\phi} E(u^k, \phi)$ `// Nearest neighbor search`
3: $u_{k+1} \leftarrow \arg\min_{u} E(u, \phi^k)$ `// Image reconstruction`
4: $k \leftarrow k + 1$
5: **until** $\|u_{k+1} - u_k\| < \tau$

For the **image reconstruction**, we reconstruct each pixel in the occluded area using a weighted mean scheme, initially proposed by Wexler et al. [51]. In particular, given fixed shift map $\phi$, the pixel at position $p \in \mathcal{H}$ is assigned the color value

$$u(p) = \frac{\sum_{q \in \mathcal{N}_p} s_q^p u(p + \phi(q))}{\sum_{q \in \mathcal{N}_p} s_q^p}, \ \forall p \in \mathcal{H}, \tag{2}$$

where $\mathcal{N}_p$ is the patch neighborhood of $p$ and the weight $s_q^p$ is indicated by the ANN of $W_q$, $s_q^p = \exp(-d^2(W_q, W_{q+\phi(q)})/(2\sigma^2))$.

Finally, since microstructure images often have structures of different sizes, ranging from large objects to fine scale textures and details, our microstructure reconstruction problem is inherently multiscale. We finish the patch-based inpainting with a **multiscale scheme**, [51, 1, 16, 34]. Here, we sequentially apply the inpainting scheme on an image pyramid, starting at the coarsest scale. The result at each scale is upsampled and used as initialization for the next finer scale. We adopt the algorithm of Newson et al. [34], which upsamples the shift map rather than the image content, and tunes the pyramid level according to the patch size and the occlusion size. For more details, we refer the interested reader to [34, 43].

## 3 Applications on UHCSDB database

In this section, we demonstrate the application of our aforementioned method to the UHCSDB [13]. Scikit-image Python package [50] is used to create a series of occlusion images, in concert with the inpainting implementation from Newson et al. [34] to solve the original image inpainting. We note that the current implementation is limited to execute sequentially on one processor, thus hindering the possibility of parallelism on high-performance computing platforms. The patch size parameter is also noted to have a strong effect on the computational time; that is, larger patch is associated with longer computational time. The culprit of the patch size parameter is described in lines 12, 15, and 16 in Algorithm 2, mainly due to the computation of patch distance, $d(\cdot, \cdot)$, which compares the values of pixels to pixels. Because the patch area scales as the square of the patch size parameter, the computational cost grows at least quadratically, which suggests a trade-off between efficiency and effectiveness in using inpainting method. To pre-process UHCSDB, original micrographs are cropped to eliminate the annotations, legends, as well as other metadata information, while retaining only the pure images. After cropping, the dimension of each micrograph is 484 pixel ×645 pixel. The dimension is consistent across the whole dataset after the pre-process.

To rigorously quantify the effectiveness of the inpainting algorithm, the occluded regions $\mathcal{H}$ are randomly created with as an ellipse with random major and minor dimensions, as well as orientation, which are shown as green ellipses. Figure 2 shows the comparison between original (left column) and reconstructed (right column) microstructures, respectively, for microstructures #35, #1098, #1294, and #1633. Figure 3 shows the comparison between original (left column) and reconstructed (right column) microstructures, respectively, for microstructures #1718, #1561, #1457, and #36. The texture in reconstructed microstructure is continuous between the occluded $\mathcal{D}$ and unoccluded regions $\mathcal{H}$. The difference within the occluded regions between original and reconstructed microstructures is obvious when comparison is shown. Without the comparison, it is visually indistinguishable and

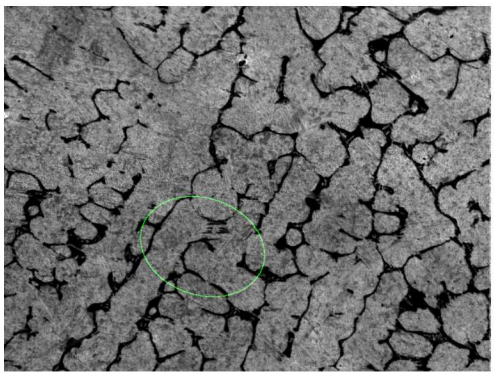

(a) Orig. #35.

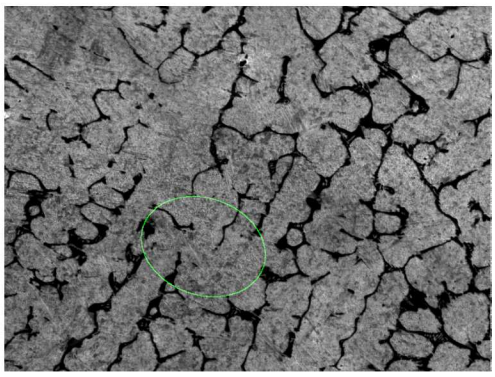

(b) Recon. #35.

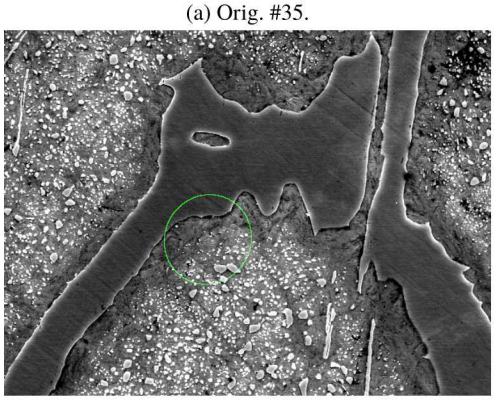

(c) Orig. #1098.

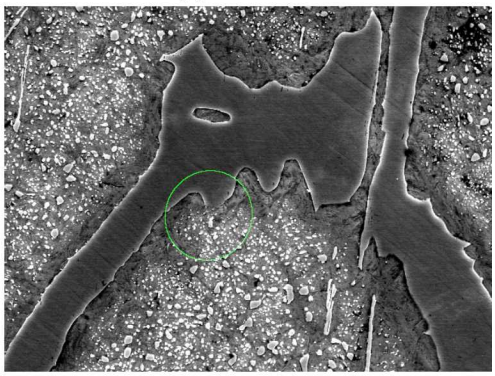

(d) Recon. #1098.

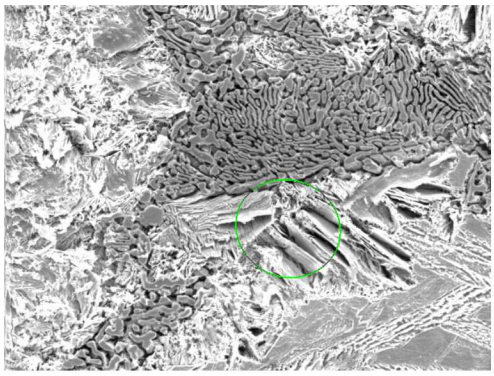

(e) Orig. #1294.

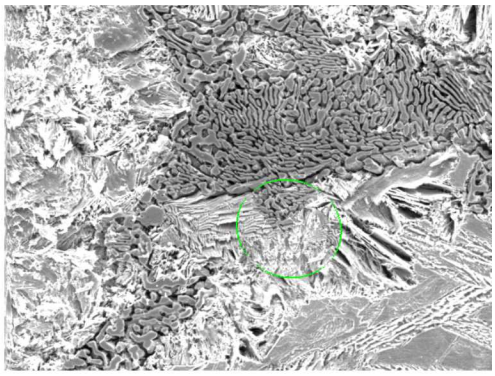

(f) Recon. #1294.

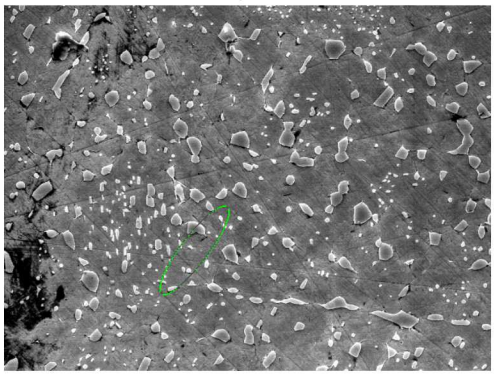

(g) Orig. #1633.

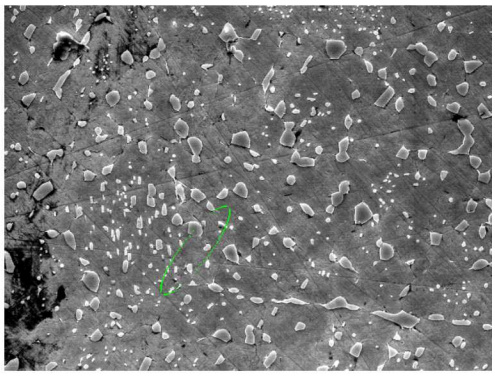

(h) Recon. #1098.

Fig. 2: Image inpainting for microstructure reconstruction. The difference is the region highlighted by the green border. Patch size of 7 pixel is used in this figure.

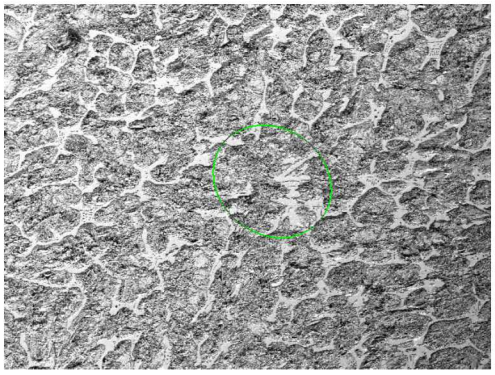

(a) Orig. #1718.

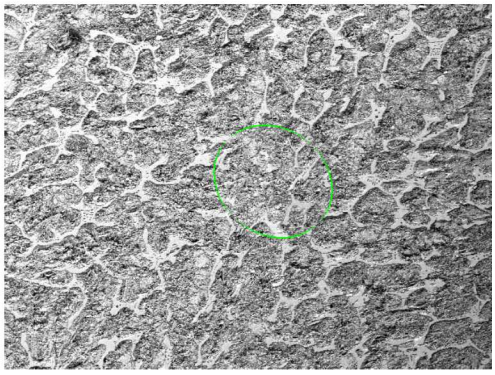

(b) Recon. #1718.

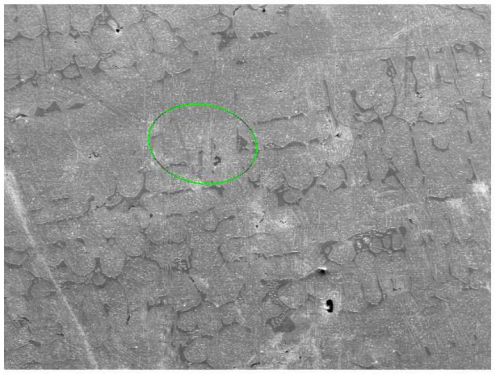

(c) Orig. #1561.

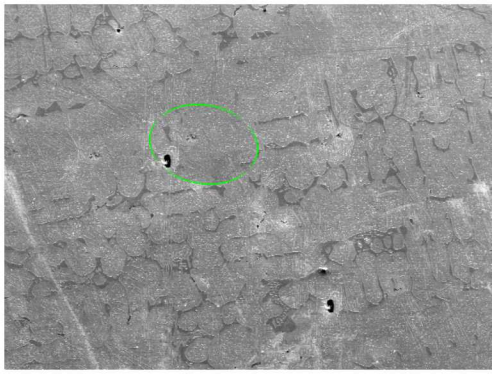

(d) Recon. #1561.

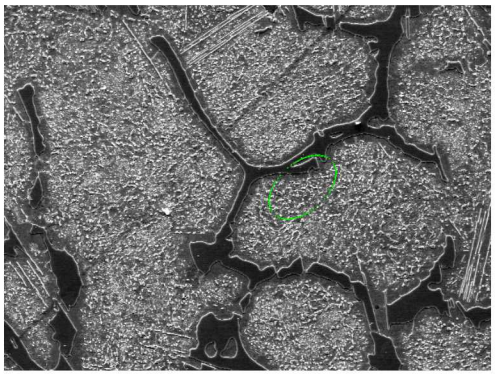

(e) Orig. #1457.

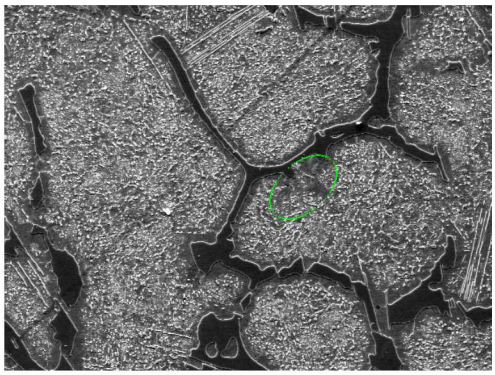

(f) Recon. #1457.

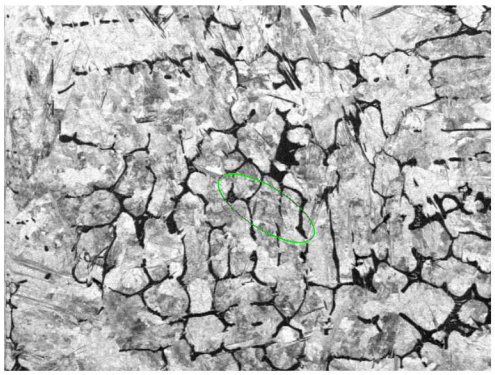

(g) Orig. #36.

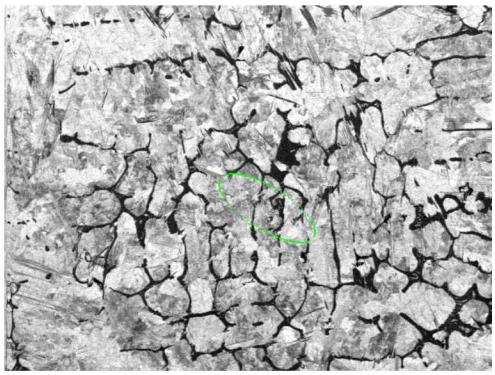

(h) Recon. #36.

Fig. 3: Image inpainting for microstructure reconstruction. The difference is the region highlighted by the green border. Patch size of 3 pixel is used in this figure.

difficult to classify if the microstructures are indeed real or fake, even for human experts. This highlights the impact of our inpainting algorithm to generate synthetic microstructures. Besides GAN, which is known to generate high-quality synthetic microstructure, our method provides an alternative option, without resorting to DL techniques.

## 4 Discussion and Conclusion

In this paper, a microstructure reconstruction framework is applied based on our previous work [43] and the image inpainting algorithm of Newson et al. [34], which extensively uses the PatchMatch algorithm from Barnes et al [3]. It is noteworthy that our approach does not suffer from the lack of data, which is a common problem in experiments, particularly for experimental materials science. However, this does not mean to compete with and to be viewed as alternatives for ML/DL approaches, such as GAN and AE, for microstructure generation and reconstruction problems. Rather, we would like to view it as a complementary approach, which can further make it easier to apply ML/DL to bridge the gap between small and big data, as ML/DL techniques are well-known to be data-hungry. Intuitively, it is equivalent to bootstrapping method in statistics, because the patches are drawn within the limited dataset $\mathcal{D}$, thus samples and microstructure features are reused.

**Algorithm 2** Approximate nearest neighbor (ANN) search using PatchMatch [3, 16]. Reprinted with permission from [43].

**Input:** Current image $u$, occlusion $\mathcal{H}$, number of iteration $J$
**Output:** Shift map $\phi$

$\phi \leftarrow$ randomly initialize the shift map
$(p_n)$, $n = 1, \ldots, |\mathcal{H}| \leftarrow$ lexicography ordering of the pixels in $\mathcal{H}$
**for** $j = 1, \ldots, J$ **do**
  **for** $n = 1, \ldots, |\mathcal{H}|$ **do**
    **if** $j$ is even **then**
      $p \leftarrow p_n$ `// visit the occluded pixels by lexicography order`
      $a \leftarrow p - (0,1)$, $b \leftarrow p - (1,0)$ `// check adjacent (up and left) pixels`
    **else**
      $p \leftarrow p_{|\mathcal{H}|-n+1}$ `// visit the occluded pixels by inverse order`
      $a \leftarrow p + (0,1)$, $b \leftarrow p + (1,0)$ `// check down and right pixels`
    **end if**
    $q \leftarrow \underset{r \in \{p,a,b\}}{\arg\min}\ d(W_p, W_{p+\phi(r)})$ `// update candidate for NNs of current pixel`
    $\phi(p) \leftarrow \phi(q)$
    `// Random search for better NNs around the current one`
    $\mathbb{S} \leftarrow$ Generate set of random 2D vectors around $\phi(p)$
    $t \leftarrow \underset{r \in \mathbb{S} \cup \{\phi(p)\}}{\arg\min}\ d(W_p, W_{p+r})$
    $\phi(p) \leftarrow t$
  **end for**
**end for**

The inpainting algorithm plays an important role in generating statistically equivalent microstructures. To this end, UQ is utilized in materials science [2] to ensure that both aleatory and epistemic uncertainty are rigorously quantified. While two-point statistics and principal component analysis are among most popular choices for quantifying uncertainty associated with microstructures, it is noted that other methods also exist, such as intervals [46], sparse grid [49], Gaussian process regression [48, 44, 40, 42], with applications to other ICME models and simulations. Inverse problems in process-structure [41] and structure-property linkages [47] have also been explored for UQ where a single forward ICME model is considered. For multiple ICME models, multi-fidelity approaches [35, 45] remain a viable option for coupling multi-physics ICME models which share some common entities.

For the microstructure reconstruction in this paper, we note that small patch size parameter is good at boundary refinement, which in turn is used to ensure the microstructural continuity between the occluded and unoccluded regions. Large patch size parameter is typically used for outpainting problems in order to avoid excessive repetition of patches. Within the scope of this study, large patch size parameter is not considered.

Compared to prior works [23, 21, 22], the image inpainting method in this paper can generate microstructures at the same fidelity of the experiments, which are the state-of-the-art in microstructure reconstruction and generation, beside ML/DL approaches. It should be also noted that there is a similar feature in the Adobe Photoshop commercial package, which is widely used in microscopy, which allows image inpainting as well. This proprietary implementation of the PatchMatch algorithm is known as "content-aware fill" operation [4] in the Adobe Photoshop package. Due to the license constraint, we did not compare the performance between our algorithm and the Adobe Photoshop package.

## Acknowledgment

The views expressed in the article do not necessarily represent the views of the U.S. Department of Energy or the United States Government. Sandia National Laboratories is a multimission laboratory managed and operated by National Technology and Engineering Solutions of Sandia, LLC., a wholly owned subsidiary of Honeywell International, Inc., for the U.S. Department of Energy's National Nuclear Security Administration under contract DE-NA-0003525. Oak Ridge National Laboratory is a multiprogram science and technology national laboratory operated by UT-Battelle, LLC., for the U.S. Department of Energy under contract DE-AC05-00OR22725.

## References

1. Arias, P., Facciolo, G., Caselles, V., Sapiro, G.: A variational framework for exemplar-based image inpainting. International journal of computer vision **93**(3), 319–347 (2011)
2. Arróyave, R., McDowell, D.L.: Systems approaches to materials design: Past, present, and future. Annual Review of Materials Research **49**(1), 103–126 (2019)
3. Barnes, C., Shechtman, E., Finkelstein, A., Goldman, D.B.: PatchMatch: A randomized correspondence algorithm for structural image editing. In: ACM Transactions on Graphics (ToG), vol. 28, p. 24. ACM (2009)
4. Bedi, A., Gupta, S., Gupta, S.: Content aware fill based on similar images (2017). US Patent 9,697,595
5. Bostanabad, R.: Reconstruction of 3D microstructures from 2D images via transfer learning. Computer-Aided Design **128**, 102906 (2020)
6. Bostanabad, R., Bui, A.T., Xie, W., Apley, D.W., Chen, W.: Stochastic microstructure characterization and reconstruction via supervised learning. Acta Materialia **103**, 89–102 (2016)
7. Cang, R., Ren, M.Y.: Deep network-based feature extraction and reconstruction of complex material microstructures. In: ASME 2016 International Design Engineering Technical Conferences and Computers and Information in Engineering Conference, pp. V02BT03A008–V02BT03A008. American Society of Mechanical Engineers (2016)
8. Cang, R., Xu, Y., Chen, S., Liu, Y., Jiao, Y., Ren, M.Y.: Microstructure representation and reconstruction of heterogeneous materials via deep belief network for computational material design. Journal of Mechanical Design **139**(7), 071404 (2017)
9. Chen, D., He, X., Teng, Q., Xu, Z., Li, Z.: Reconstruction of multiphase microstructure based on statistical descriptors. Physica A: Statistical Mechanics and its Applications **415**, 240–250 (2014)
10. Chen, S., Kirubanandham, A., Chawla, N., Jiao, Y.: Stochastic multi-scale reconstruction of 3d microstructure consisting of polycrystalline grains and second-phase particles from 2d micrographs. Metallurgical and Materials Transactions A pp. 1440–1450 (2016)
11. Chun, S., Roy, S., Nguyen, Y.T., Choi, J.B., Udaykumar, H., Baek, S.S.: Deep learning for synthetic microstructure generation in a materials-by-design framework for heterogeneous energetic materials. arXiv preprint arXiv:2004.04814 (2020)
12. DeCost, B.L., Francis, T., Holm, E.A.: Exploring the microstructure manifold: Image texture representations applied to ultrahigh carbon steel microstructures. Acta Materialia **133**, 30–40 (2017)
13. DeCost, B.L., Hecht, M.D., Francis, T., Webler, B.A., Picard, Y.N., Holm, E.A.: UHCSDB: Ultrahigh carbon steel micrograph database. Integrating Materials and Manufacturing Innovation **6**(2), 197–205 (2017)
14. DeCost, B.L., Lei, B., Francis, T., Holm, E.A.: High throughput quantitative metallography for complex microstructures using deep learning: a case study in ultrahigh carbon steel. arXiv preprint arXiv:1805.08693 (2018)
15. van Der Maaten, L.: Accelerating t-SNE using tree-based algorithms. The Journal of Machine Learning Research **15**(1), 3221–3245 (2014)
16. Fedorov, V., Facciolo, G., Arias, P.: Variational framework for non-local inpainting. Image Processing On Line **5**, 362–386 (2015)
17. Feng, J., Li, C., Cen, S., Owen, D.: Statistical reconstruction of two-phase random media. Computers & Structures **137**, 78–92 (2014)
18. Fullwood, D., Kalidindi, S., Niezgoda, S., Fast, A., Hampson, N.: Gradient-based microstructure reconstructions from distributions using fast fourier transforms. Materials Science and Engineering: A **494**(1-2), 68–72 (2008)
19. Fullwood, D.T., Niezgoda, S.R., Kalidindi, S.R.: Microstructure reconstructions from 2-point statistics using phase-recovery algorithms. Acta Materialia **56**(5), 942–948 (2008)
20. Goodfellow, I., Pouget-Abadie, J., Mirza, M., Xu, B., Warde-Farley, D., Ozair, S., Courville, A., Bengio, Y.: Generative adversarial nets. In: Advances in Neural Information Processing Systems, pp. 2672–2680 (2014)
21. Groeber, M., Ghosh, S., Uchic, M.D., Dimiduk, D.M.: A framework for automated analysis and simulation of 3D polycrystalline microstructures. Part 1: Statistical characterization. Acta Materialia **56**(6), 1257–1273 (2008)
22. Groeber, M., Ghosh, S., Uchic, M.D., Dimiduk, D.M.: A framework for automated analysis and simulation of 3D polycrystalline microstructures. Part 2: Synthetic structure generation. Acta Materialia **56**(6), 1274–1287 (2008)
23. Groeber, M., Uchic, M., Dimiduk, D., Bhandari, Y., Ghosh, S.: A framework for automated 3d microstructure analysis & representation. Journal of Computer-Aided Materials Design **14**(1), 63–74 (2007)
24. Iyer, A., Dey, B., Dasgupta, A., Chen, W., Chakraborty, A.: A conditional generative model for predicting material microstructures from processing methods. arXiv preprint arXiv:1910.02133 (2019)
25. Latief, F., Biswal, B., Fauzi, U., Hilfer, R.: Continuum reconstruction of the pore scale microstructure for fontainebleau sandstone. Physica A: Statistical Mechanics and its Applications **389**(8), 1607–1618 (2010)
26. Li, D., Sun, X., Khaleel, M.: Comparison of different upscaling methods for predicting thermal conductivity of complex heterogeneous materials system: application on nuclear waste forms. Metallurgical and Materials Transactions A **44**(1), 61–69 (2013)

27. Li, D., Tschopp, M.A., Khaleel, M., Sun, X.: Comparison of reconstructed spatial microstructure images using different statistical descriptors. Computational Materials Science **51**(1), 437–444 (2012)
28. Li, X., Zhang, Y., Zhao, H., Burkhart, C., Brinson, L.C., Chen, W.: A transfer learning approach for microstructure reconstruction and structure-property predictions. Scientific reports **8**(1), 1–13 (2018)
29. Ling, J., Hutchinson, M., Antono, E., DeCost, B., Holm, E.A., Meredig, B.: Building data-driven models with microstructural images: Generalization and interpretability. Materials Discovery **10**, 19–28 (2017)
30. Liu, Y., Caselles, V.: Exemplar-based image inpainting using multiscale graph cuts. IEEE transactions on image processing **22**(5), 1699–1711 (2013)
31. van der Maaten, L., Hinton, G.: Visualizing data using t-SNE. Journal of machine learning research **9**(Nov), 2579–2605 (2008)
32. Mosser, L., Dubrule, O., Blunt, M.J.: Reconstruction of three-dimensional porous media using generative adversarial neural networks. Physical Review E **96**(4), 043309 (2017)
33. Newson, A., Almansa, A., Fradet, M., Gousseau, Y., Pérez, P.: Video inpainting of complex scenes. SIAM Journal on Imaging Sciences **7**(4), 1993–2019 (2014)
34. Newson, A., Almansa, A., Gousseau, Y., Pérez, P.: Non-local patch-based image inpainting. Image Processing On Line **7**, 373–385 (2017)
35. Peherstorfer, B., Willcox, K., Gunzburger, M.: Survey of multifidelity methods in uncertainty propagation, inference, and optimization. SIAM Review **60**(3), 550–591 (2018)
36. Simonyan, K., Zisserman, A.: Very deep convolutional networks for large-scale image recognition. arXiv preprint arXiv:1409.1556 (2014)
37. Singh, R., Shah, V., Pokuri, B., Sarkar, S., Ganapathysubramanian, B., Hegde, C.: Physics-aware deep generative models for creating synthetic microstructures. arXiv preprint arXiv:1811.09669 (2018)
38. Staraselski, Y., Brahme, A., Mishra, R., Inal, K.: Reconstruction of the 3D representative volume element from the generalized two-point correlation function. Modelling and Simulation in Materials Science and Engineering **23**(1), 015007 (2014)
39. Stickel, J.J.: Data smoothing and numerical differentiation by a regularization method. Computers & chemical engineering **34**(4), 467–475 (2010)
40. Tran, A., He, L., Wang, Y.: An efficient first-principles saddle point searching method based on distributed kriging metamodels. ASCE-ASME Journal of Risk and Uncertainty in Engineering Systems, Part B: Mechanical Engineering **4**(1), 011006 (2018)
41. Tran, A., Mitchell, J.A., Swiler, L.P., Wildey, T.: An active-learning high-throughput microstructure calibration framework for process-structure linkage in materials informatics. Acta Materialia **194**, 80–92 (2020)
42. Tran, A., Sun, J., Furlan, J.M., Pagalthivarthi, K.V., Visintainer, R.J., Wang, Y.: pBO-2GP-3B: A batch parallel known/unknown constrained Bayesian optimization with feasibility classification and its applications in computational fluid dynamics. Computer Methods in Applied Mechanics and Engineering **347**, 827–852 (2019)
43. Tran, A., Tran, H.: Data-driven high-fidelity 2D microstructure reconstruction via non-local patch-based image inpainting. Acta Materialia **178**, 207–218 (2019)
44. Tran, A., Tran, M., Wang, Y.: Constrained mixed-integer Gaussian mixture Bayesian optimization and its applications in designing fractal and auxetic metamaterials. Structural and Multidisciplinary Optimization pp. 1–24 (2019)
45. Tran, A., Tranchida, J., Wildey, T., Thompson, A.P.: Multi-fidelity machine-learning with uncertainty quantification and Bayesian optimization for materials design: Application to ternary random alloys. The Journal of Chemical Physics **153**, 074705 (2020)
46. Tran, A., Wang, Y.: A molecular dynamics simulation mechanism with imprecise interatomic potentials (May 31 - June 4, 2015). The 3rd TMS World Congress on Integrated Computational Materials Engineering (ICME 2015), Colorado Springs, CO
47. Tran, A., Wildey, T.: Solving stochastic inverse problems for property-structure linkages using data-consistent inversion and machine learning. JOM (2020)
48. Tran, A., Wildey, T., McCann, S.: sMF-BO-2CoGP: A sequential multi-fidelity constrained Bayesian optimization for design applications. Journal of Computing and Information Science in Engineering **20**(3), 1–15 (2020)
49. Tran, A.V., Liu, D., Tran, H.A., Wang, Y.: Quantifying uncertainty in the process-structure relationship for Al-Cu solidification. Modelling and Simulation in Materials Science and Engineering **27**(6), 064005 (2019)
50. Van der Walt, S., Schönberger, J.L., Nunez-Iglesias, J., Boulogne, F., Warner, J.D., Yager, N., Gouillart, E., Yu, T.: scikit-image: Image processing in Python. PeerJ **2**, e453 (2014)
51. Wexler, Y., Shechtman, E., Irani, M.: Space-time completion of video. IEEE Transactions on Pattern Analysis & Machine Intelligence (3), 463–476 (2007)
52. Xu, H., Dikin, D.A., Burkhart, C., Chen, W.: Descriptor-based methodology for statistical characterization and 3d reconstruction of microstructural materials. Computational Materials Science **85**, 206–216 (2014)
53. Xu, H., Liu, R., Choudhary, A., Chen, W.: A machine learning-based design representation method for designing heterogeneous microstructures. Journal of Mechanical Design **137**(5), 051403 (2015)
54. Zinchenko, A.Z.: Algorithm for random close packing of spheres with periodic boundary conditions. Journal of Computational Physics **114**(2), 298–307 (1994)